Subproject E1.01

Novel Carriers for Nano-Structured Material Through Membranes

Principle Investigators: Stefan Bräse

CFN-Financed Scientists:

Further Scientists: Dr. Daniel Fritz, Dr. Esther Birtalan, Dr. Frank Hahn, Dr. Ute Schepers, Birgit Rudat, Carmen Cardenal, Daniel Fürniß, Dominik Kölmel, Sidonie Vollrath

Institute of Organic Chemistry
Karlsruhe Institute of Technology (KIT)

E1.01 Bräse

Novel Carriers for Nano-Structured Material Through Membranes

Introduction and Summary

The design of new biochemical and physical cellular modulators has ever been limited by the question of bioavailability. Most pharmaceutically active molecules or functional particles do not fulfill the necessary criteria for cellular uptake and bioavailability. In classical terms, cellular uptake is limited to a small number of structures that can either penetrate the hydrophobic biological membrane barrier due to their physical properties or are recognized by cellular transport systems. Biological membranes, which surround every cell, consist of a lipid bilayer that serves as structural scaffold for functionally active proteins. According to the "fluid mosaic model", a membrane is a highly dynamic assembly of various kinds of lipids (e.g. phospholipids, sphingolipids, cholesterol). It provides a two-dimensional matrix in which integral membrane proteins are able to move around. Under physiological conditions, all membrane lipids are amphipathic molecules. They aggregate spontaneously into a bilayer, where the fatty acyl chains are clustered within the hydrophobic interior insulated by the polar heads that face the aqueous environment. The delivery of cargo across the membrane has to be triggered by specific mechanisms. Cellular uptake occurs either *via* undirected passive or by directed active membrane transport. The latter includes directed or undirected endocytosis, and classical import via channels and pore-forming proteins or receptors.
During the last funding period the cellular uptake of nanoparticles was investigated using native and designed molecular transporters. In a collaborative effort using chemical, biochemical, physical and spectroscopic methods, novel transporters were designed, synthesized, and characterized. Their role and function in the cellular uptake of nanostructured materials were determined.
The research area Nano-Biology addresses the interactions between living cells and inanimate materials at the molecular level, with the aim to functionalize or manipulate cells by these materials. An emphasis lies in the directed transport of nanoparticles through cellular membranes and in the adhesion of cells on nanostructured surfaces.
The specific goals of *subproject E1* for the last funding period were:

- Application and improvement of the use of cell penetrating macromolecules for delivering nanoparticles into living cells. In particular, bioconjugation methods such as "click" reactions of azides and alkynes should be improved.[1]
- Preparation of suitable synthetic carriers, loading them with relevant nano-cargo, characterizing their structures in biological membranes, and monitoring the delivery of the cargo into the cell.
- Transport those nanomaterials into cells, which are available from research areas C and D, such as magnetic clusters, nanotubes, quantum dots, chromophores, inorganic biomimetics, amongst others. The special physicochemical features of these compounds will allow their manipulation from the cellular exterior by means of magnetic or electric fields, heat or illumination, thereby exerting a physical force within the cell or releasing bioactive compounds at a targeted site.
- Assessing the toxicity and cellular response to novel types and different sizes of cargo [2], and correlation of the physico-chemical properties of nanoparticles with their uptake by special cell types and possible accumulation within specific organelles.

1. Synthesis of Molecular Transporters

The cellular membrane consists of a lipid bilayer and is impermeable to hydrophilic molecules and to particles of nanoscopic dimensions. Hence, for therapeutic or biotechnological purposes there

exists no straightforward route to deliver pharmaceutically active agents into cells. Over the recent years, however, several small peptides have been discovered that are able to translocate across the plasma membrane in an energy-independent way. These cell-penetrating peptides (CPPs), also called "Trojan" peptides, offer a promising route to deliver any desired cargo into cells. They are known to be able to transport many types of otherwise inaccessible cargos across cellular membranes without causing cellular leakage. They are currently being applied in the pharmaceutical industry for depositing biologically active compounds (drugs, proteins, siRNA, DNA, etc.) into cells.
Since the functional mechanism of the Trojan transport phenomenon is not yet understood, some better structural insights of the transport peptides and polymers helped to develop more efficient and more selective transporters. During the last funding period they could be optimized for nanoscopic and non-biological cargo. Many questions such as the size-relationships were explored. Furthermore, the cellular responses to such alien materials were characterized toxicologically, with a view to potential health risks and prospective medical applications. The groups worked hand in hand to build a bridge from synthesis (Bräse, Ulrich) and structure analysis (Ulrich, Lemmer) to the biological (Krug, [3,9] Bräse, Nick, [11] Wedlich, Bastmeyer) and microscopic (Lemmer, Naber, Schimmel) characterization and application of these coupled bio-nano-materials.

1.1. Polyamine Transporters

In preliminary studies, polyamines have been shown to be useful as molecular transporters. In order to improve the uptake and activity of polyamines, new polyamines and strategies for their synthesis and modification are needed. We were trying to reach these goals in several different approaches. The advantages of solid phase synthesis for making desired compounds, which were shown in previous studies, led to most syntheses being carried out in this manner. Additionally, the already established protecting group strategy was used.
In one approach, two methods for the build-up of polyamines on the resin were compared. With each method, a tetraamine was synthesized starting with a diamine using FUKUYAMA and FUKUYAMA-MITSUNOBU alkylation, respectively. These two methods opened up the possibility of modifying every single sidechain on the nitrogen individually as well as alternating the number of CH_2 groups in between the amino groups under mild conditions.
In another approach, hydroboration as a method for functionalizing polyamines was investigated. For this method, an alkene residue was added to the polyamine through FUKUYAMA alkylation. After hydroboration of the alkene, the borane was turned into various functional groups. It was shown that the boranes react with α-haloesters, undergo the SUZUKI reaction and can be converted into alcohols. To test the versatility of this method, the hydroboration was carried out on four alkene residues with a different substitution pattern and with two different hydroboration agents.

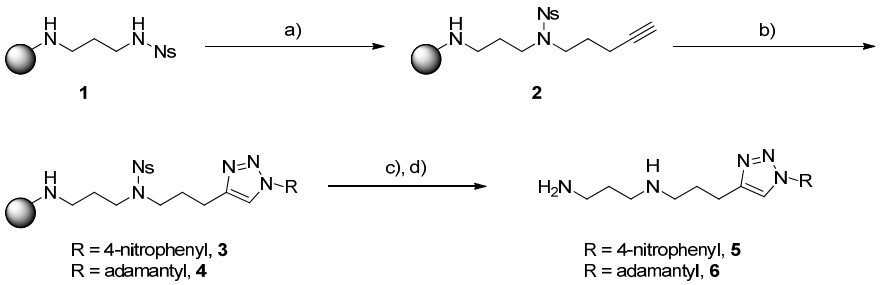

Scheme 1: Synthesis of polyamine conjugates *via* click chemistry. Reaction conditions: a) 5-chloropent-1-yne, potassium carbonate in DMF, 60 °C, 2 d; b) 4-nitrophenylazide or adamantylazide, copper(I) iodide, DIPEA in absolute THF, rt, 18 h; c) 2-mercaptoethanol, DBU in DMF, rt, 2 d; d) 5% TFA in CH_2Cl_2, rt, 18 h.

Furthermore, the click reaction was applied on solid-phase polyamine synthesis (**Fehler! Verweisquelle konnte nicht gefunden werden.**). To this purpose an alkyne group was introduced to an immobilized diamine through FUKUYAMA alkylation. Using two electronically as well as sterically different azides as an example, it was demonstrated that the click reaction is easily accessible. The widely different azides also showed the versatility of this conjugation method. The reaction was also compatible with the used protection group and was carried out under mild conditions. In further studies, these preliminary results can be applied on larger polyamines and their conjugation to active structures, such as dyes, bio-markers, drugs, etc.

1.2. Peptoid Transporters

Based on synthetic oligomers such as polyamines and peptoids, which have been shown to be efficient and inexpensive drug carriers, the group of S. Bräse developed novel transporters. [3,9] We continued to optimize the delivery of nanoparticles (for example non-soluble fluorophores or porphyrines) into cells and got a better understanding of the carriers functional mechanism. This was an integral part in the collaboration of the group S. Bräse (E1.01) with the groups of A. Ulrich (E1.02) [9] and U. Lemmer (E1.04).
Peptoids are very similar to peptides with the distinction that the side chains are formally shifted from the α–carbon atom to the adjacent nitrogen atom. Since peptoids are nearly unknown in nature, they show a greater stability against enzymatic degradation in comparison with the corresponding peptides. Therefore, they are more suitable as molecular transporters than CPPs.
In particular we used combinatorial synthetic methods and high-throughput techniques such as solid-phase synthesis to prepare novel transporters (**Fehler! Verweisquelle konnte nicht gefunden werden.**).

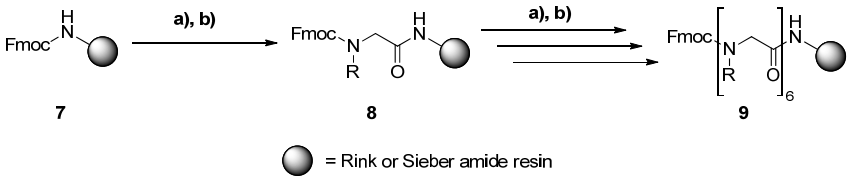

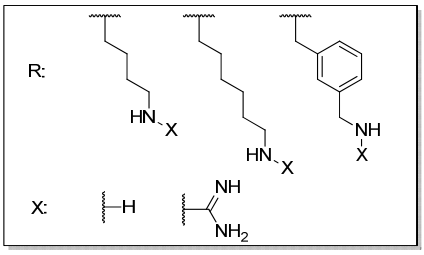

Scheme 1: General procedure for the solid phase synthesis of resin bond peptoid hexamers. Reaction conditions: a) 20% piperidine in DMF, 3 x 5 min; b) 3.00 eq monomer, 3.00 eq DIC, 3.00 eq HOBt×H_2O in DMF, mw, 60 °C, 30 min (double coupling).

1.3. Conjugation with Functionalized Nanostructures

For a better understanding of the cellular uptake mechanism, peptoids were labeled with two different fluorescence dyes. Between these two dyes a fluorescence resonance energy transfer (FRET) should occur. At first a relatively simple test system was synthesized (Scheme 3). The FRET donor was either 5(6)-carboxyfluorescein (CF) or 7-nitrobenz-2-oxa-1,3-diazolyl (NBD), the FRET acceptor was rhodamine B (RhB) in both cases. To distinguish between the amine on the backbone and the one on the side chain, the submonomer method (Scheme 3, conditions a) and b))

was used. Additionally, this allows us a minimal use of protecting groups. After introduction of mono-Fmoc-protected hexamethylendiamine a difunctionalization was possible. At first rhodamine B was coupled to the backbone and afterwards the Fmoc protection group was cleaved in order to attach the second dye, NBD-Cl or 5(6)-carboxyfluorescein. After the final cleavage two FRET transporters **13** and **14**, respectively, were obtained.

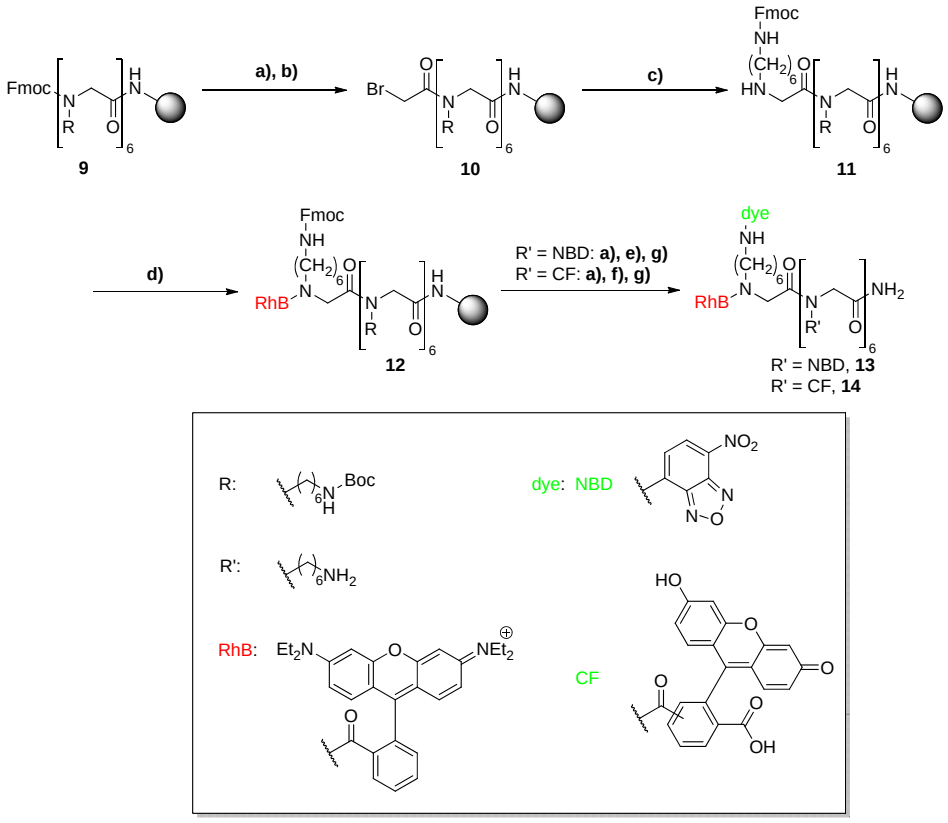

Scheme 3: Solid phase synthesis of peptoids and attachment of the two FRET dyes. The synthesis of the immobilized hexamer **9** is shown in Scheme 2. Reaction conditions: a) 20% piperidine in DMF, 3 x 5 min; b) 7.90 eq bromoacetic acid, 7.90 eq DIC in DMF, mw, 35 °C, 1 min; c) 7.90 eq Fmoc-hexamethylenediamine in DMF, mw, 60 °C, 15 min; d) 3.00 eq rhodamine B, 3.00 eq DIC, 3.00 eq HOBt×H_2O in DMF, mw, 60 °C, 30 min (double coupling); e) 3.00 eq NBD-Cl in DMF, mw, 60 °C, 30 min (double coupling); f) 3.00 eq 5(6)-carboxyfluorescein, 3.00 eq DIC, 3.00 eq HOBt×H_2O in DMF, mw, 60 °C, 30 min (double coupling); g) 50% TFA in CH_2Cl_2, rt, 12 h.

The peptoids **13** and **14** were synthesized to evaluate if the claimed FRET mechanism occurs and if we are able to track it *in vivo*. Once this was ensured, we proceeded with the synthesis of a disulfide-containing FRET transporter. Disulfides are very interesting because they can be cleaved reductively. If the disulfide bond is in between the two FRET dyes, the absence of the energy transfer would proof the cleavage. Furthermore, it is known that the cytosol is a reductive environment. It is possible to get some information about the uptake mechanism, depending on whether the mentioned energy transfer will still be observed or not, through the use of cleavable FRET transporters system.

For the synthesis of the cleavable FRET system a directed disulfide exchange should be applied. Therefore the Mmt protected thiol **16** and the activated thiol **17** were synthesized from cysteamine hydrochloride (**15**) (Scheme 4). Next, NBD-Cl was coupled to the activated thiol **17**.

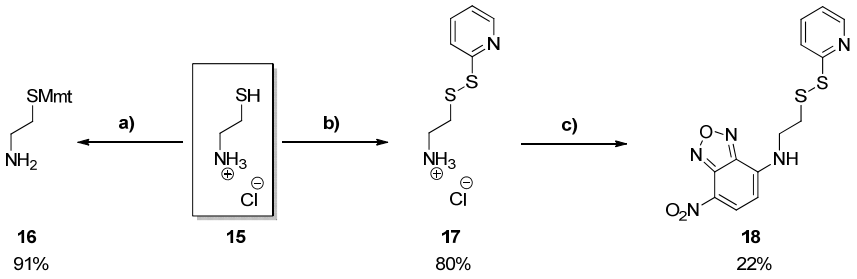

Scheme 4: Synthesis of the Mmt protected cysteamin (**16**) and the activated thiol **18**. Reaction conditions: a) 0.95 eq MmtCl in TFA, rt, 3 h; b) 2.00 eq dithiobispyridine, 1.05 eq AcOH, in MeOH, rt, 48 h; c) 1.00 eq NBD-Cl, NaOH, H_2O in EtOH, rt, 3 h.

In the same manner as described before, an immobilized hexamer was synthesized. Next, the Mmt-protected cysteamine (**16**) was introduced using the submonomer approach (Scheme 5). Afterwards rhodamine B was attached to the backbone. At the end, the Mmt protecting group was removed so that the disulfide exchange with **18** can be achieved.

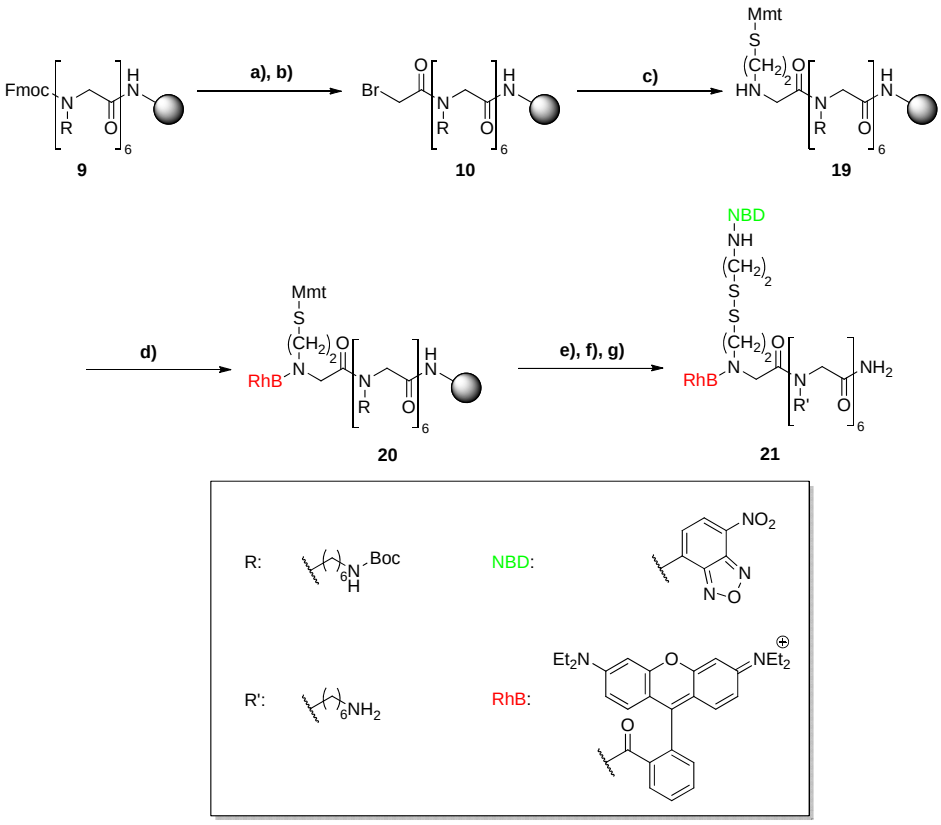

Scheme 5: Solid phase synthesis of a peptoid with cleavable FRET system. The synthesis of the immobilized hexamer **9** is shown in Scheme 2. Reaction conditions: a) 20% piperidine in DMF, 3 x 5 min; b) 7.90 eq bromoacetic acid, 7.90 eq DIC in DMF, mw, 35 °C, 1 min; c) 7.90 eq Mmt-cysteamin (**16**) in DMF, mw, 60 °C, 15 min; d) 3.00 eq rhodamine B, 3.00 eq DIC, 3.00 eq HOBt×H_2O in DMF, mw, 60 °C, 30 min (double coupling); e) 3% TFA, 7.5% TIPS in CH_2Cl_2, rt, 5 x 20 min; f) 3.00 eq activated thiol **18**, 3.00 eq DIPEA in DMF, rt, 1 h; g) 50% TFA in CH_2Cl_2, rt, 12 h.

Another project addressed the examination of lanthanide ions as possible biomarkers. To bind the lanthanide ions to the molecular transporters, we used the diethylenetriaminepentaacetic acid (DTPA) ligand. This ligand is well known for forming very stable complexes with every trivalent lanthanide ion. After the synthesis of the polymer bound hexamer **9**, the DTPA moiety is introduced

during a reaction with the commercially available DTPA dianhydride (Scheme 6). Since the two reactive sides of DTPA dianhydride are equal, this reaction generates the two different DTPA-containing transporters **22** and **23**. The complexes from these two DTPA transporters with all trivalent lanthanides (except promethium, which we didn't use due to its radioactivity) were characterized by MALDI-TOF-MS. By using the non-acidic matrix 2',4',6'-trihydroxyacetophenone, which does not cause any leakage of metal ions, all the complexes proved to be stable under the mass spectrometry conditions.

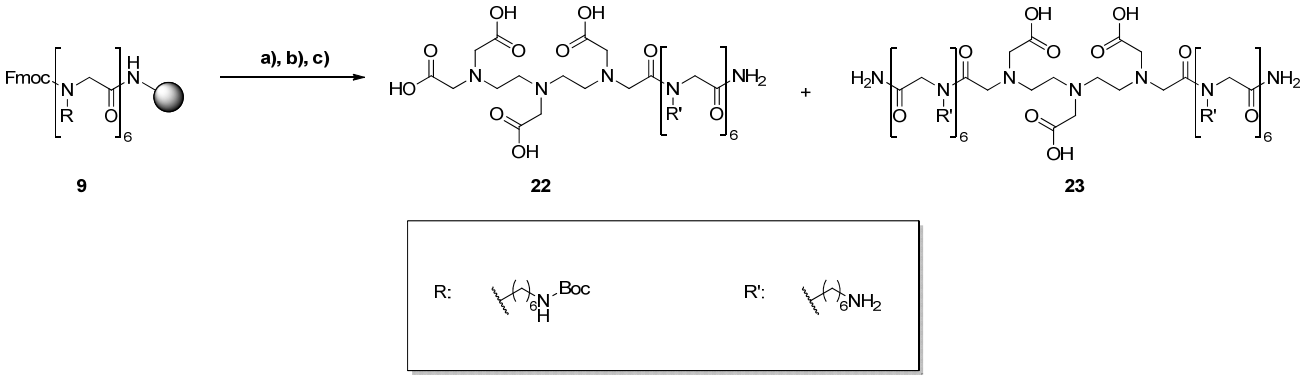

Scheme 6: Solid phase synthesis of two lanthanide complexing peptoids. The synthesis of the immobilized hexamer **9** is shown in Scheme 2. Reaction conditions: a) 20% piperidine in DMF, 3 x 5 min; b) 3.00 eq DTPA dianhydride in DMF, mw, 60 °C, 30 min (double coupling); c) 50% TFA in CH_2Cl_2, rt, 12 h.

2. Photophysical Evaluations

One of our basic approaches is to visualize peptoid-conjugated nanostructures at molecular scale. For this reason several different dyes were tested in order to find one suitable for single-molecule experiments. The use of the pyridinium dye labeled peptoid **24** made imaging and analyzing of single molecules in a poly(methyl methacrylate) (PMMA) gel possible (Figure 1). [22]

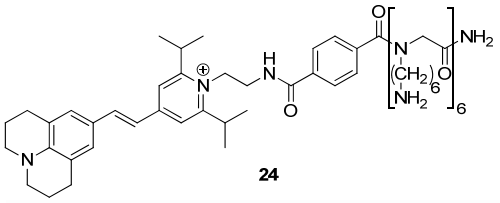

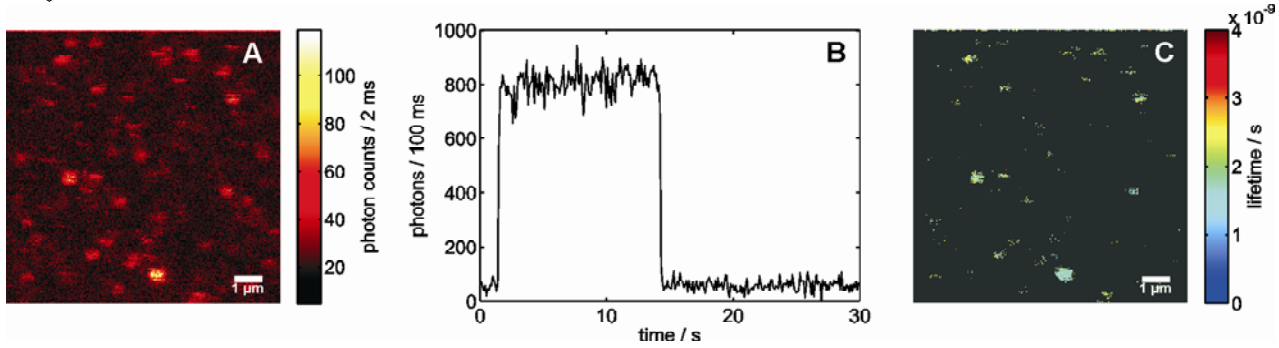

Figure 1: A: Fluorescence image of single copies (c = 10 nM) of fluorescently-labeled peptoids **24** in PMMA. B: Fluorescence intensity as a function of time for a single peptoid molecule. C: Fluorescence lifetime image of the same area as in A.

Furthermore, every FRET transporter was well examined. Since the FRET mechanism depends on several parameters, like the distance between the dyes, orientation of the transition dipole moment

etc., it is important to control whether the claimed energy transfer occurs or not (Figure 2). The mere presence of two suitable FRET dyes is just a necessary but not a sufficient condition. The FRET transporters **13** and **14** revealed a FRET efficiency of 92% and 97%, respectively.

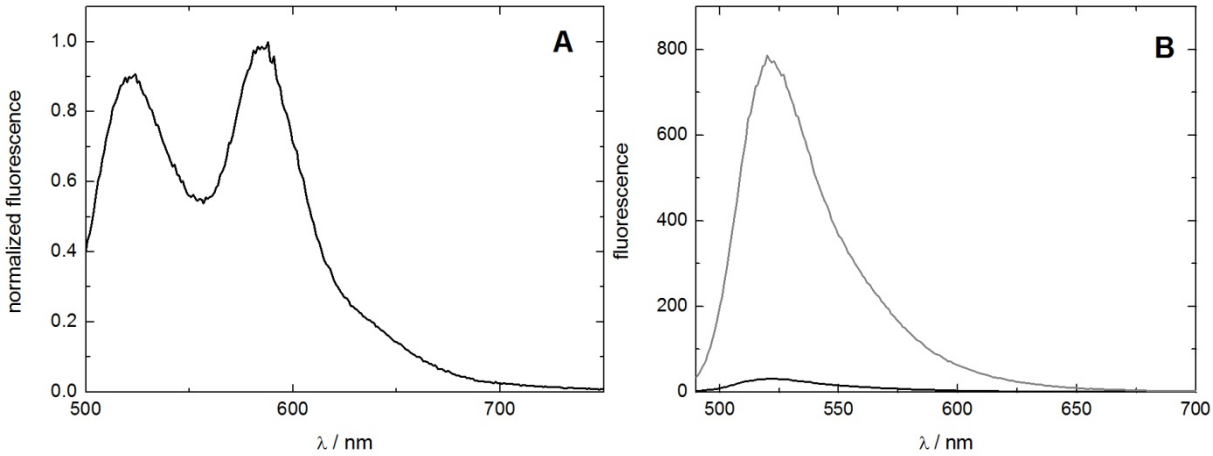

Figure 2: A: Transporter **14** in water excited with 470 nm (excitation wavelength for the donor dye). Normalized fluorescence spectrum of **14** clearly shows maxima of the donor and the acceptor. B: Comparison of fluorescence for transporter **14** (black) and a peptoid with only the donor dye. The reduced intensity of **14** is another demonstration of the occurring FRET mechanism.

One further goal was to test how the four luminescent lanthanide ions (Sm^{3+}, Eu^{3+}, Tb^{3+}, Dy^{3+}) are affected by the complexation with the two DTPA transporters **22** and **23**. In every case the peptoid complexes showed better luminescence properties than the free lanthanide ions (Figure 3). As known from the literature especially Eu^{3+} and Tb^{3+} showed a distinct luminescence, whereas the luminescence of Sm^{3+} and Dy^{3+} is less eminent. Altogether we will focus our further experiments on the Eu^{3+} and Tb^{3+} complexes with the peptoid **22** or derivatives thereof.

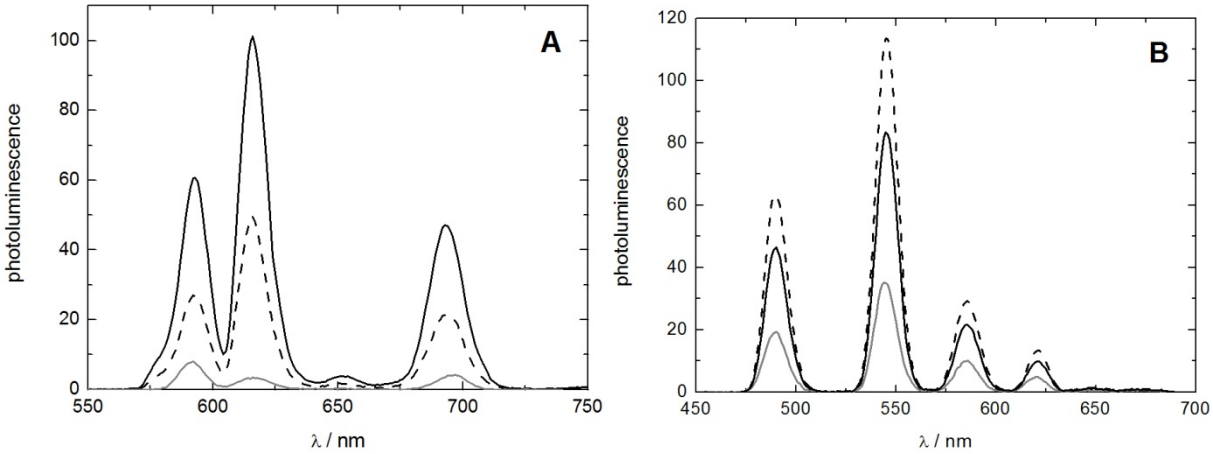

Figure 3: Time-resolved emission spectra of lanthanide DTPA-complexes in water. Grey: free salt. Black: complex with **22**. Black dashed: complex with **23**. A: Eu^{3+} salt and complexes, excited with 394 nm. B: Tb^{3+} salt and complexes, excited with 369 nm.

3. Biological Evaluations

In the CFN a wide range of nanoparticles with an even wider range of physical and chemical properties are available. Their many different potential uses as nano-tools were explored. One goal of *subproject E1* was to deliver these compounds into living cells. It is still envisaged in the long-term to influence cells with magnetic fields via magnetic clusters, to connect several cells conductively via nanotubes, to release biochemically active compounds by illumination via

photoactive chromophores, or to track the path of a particle through the cellular interior *via* optical markers such as dyes or quantum dots.

3.1. Transport into eukaryotes

Cell biological assays to monitor the transport of functionalized nanoparticles are performed with various types of living cells (HeLa, fibroblasts, COS cells, neuronal cells, epithelial cells) by the groups of H. Krug (E1.03), [3,9] P. Nick (E1.05), [11] D. Wedlich (E2.02), M. Bastmeyer (E2.03), and in cooperation with U. Schepers (Institute of Toxicology and Genetics at campus north). We measured the penetration efficiency of molecular transporters and their effect on the morphology on the cell. For this purpose we used fluorescence microscopy techniques with living cells. We monitored the accumulation of internalized nanoparticles within specific organelles or compartments, and explored the mechanisms and parameters relevant for specific targeting.

To prove that the concept of the FRET transporters is working *in vivo*, we tested the transporters **13** and **14** on HeLa cells (Figure 4 and Figure 5). As the photophysical studies indicated before, the FRET effect was seen in both cases. If the sample was illuminated with a wavelength of 488 nm a green (donor) and a red (acceptor) fluorescence signal could be detected, which were colocalized. This is due to the fact, that the energy transfer is not quantitative. By illuminating the acceptor (rhodamine B) directly with a wavelength of 561 nm only the red signal can be detected, which is consistent to our expectations. Especially the FRET transporter **13** showed a strong acceptor signal (Figure 5 B), compared to the rather weak donor signal (Figure 5 A). In the near future the cleavable FRET transporter **21** will be tested.

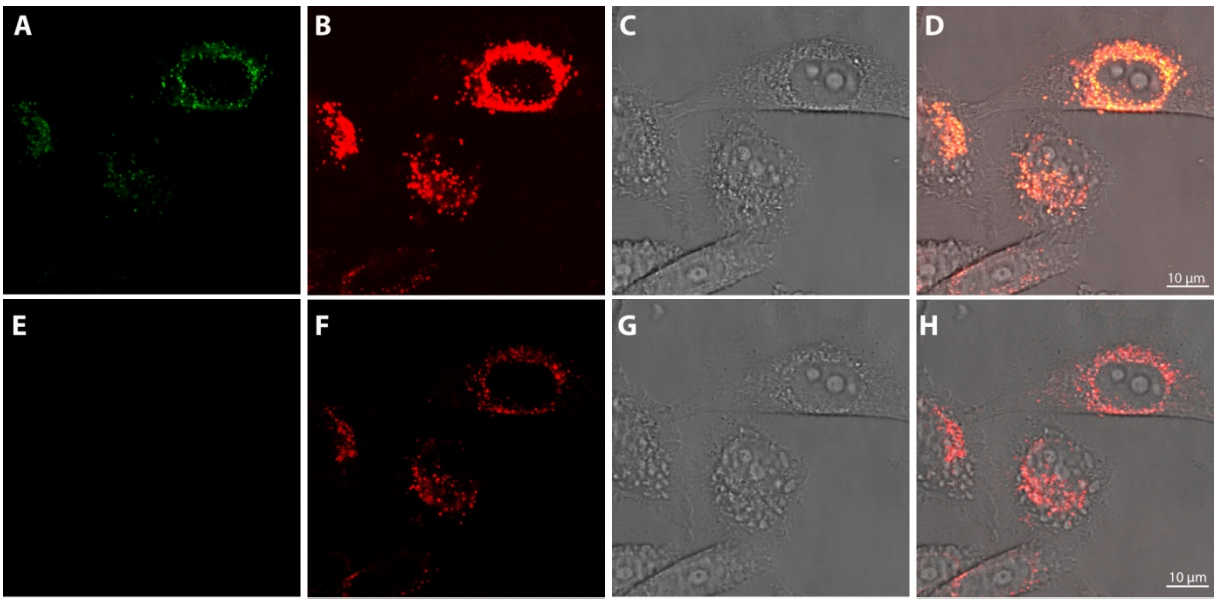

Figure 4: Confocal analysis of FRET transporter **13**. HeLa cells were incubated with **13** (15 µM) for 24 h at 37 °C. The FRET effect was visualized by confocal microscopy with an excitation wavelength of 488 nm (argon laser) (A-D) and an excitation wavelength of 561 nm (DPSS laser) (E-H). The emission was detected between 503-540 nm (5(6)-carboxyfluorescein) (A, E) and 600-678 nm (rhodamine B) (B, F). D is the overlay from A-C and H is the overlay from E-G.

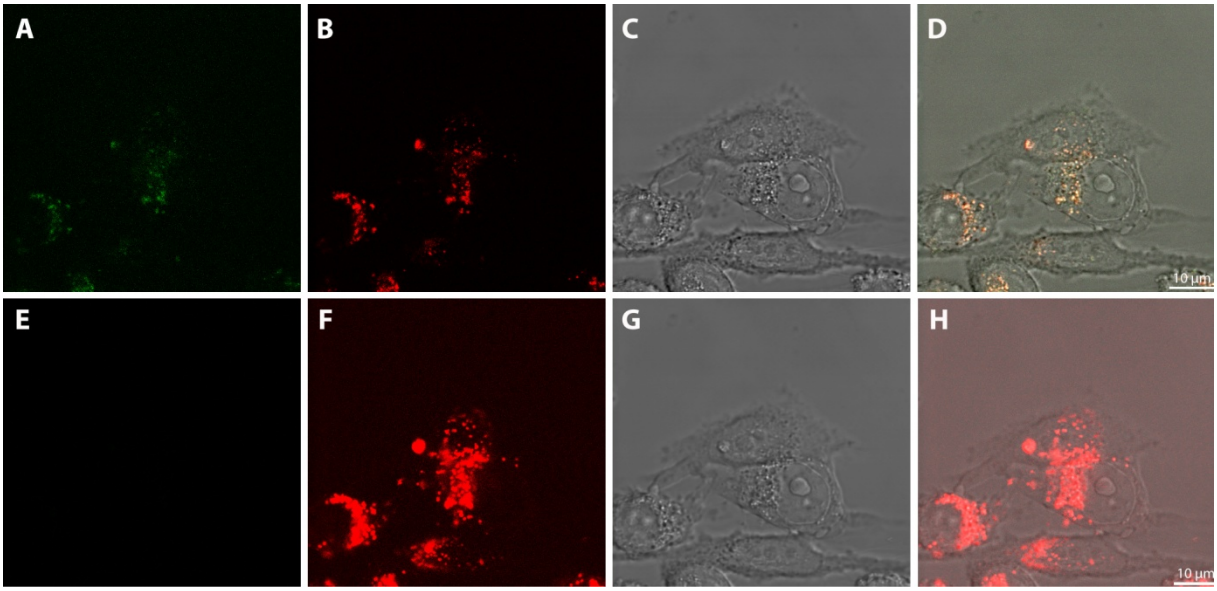

Figure 5: Confocal analysis of FRET transporter **14**. HeLa cells were incubated with **14** (15 µM) for 24 h at 37 °C. The FRET effect was visualized by confocal microscopy with an excitation wavelength of 488 nm (argon laser) (A-D) and an excitation wavelength of 561 nm (DPSS laser) (E-H). The emission was detected between 503-540 nm (NBD) (A, E) and 600-678 nm (rhodamine B) (B, F). D is the overlay from A-C and H is the overlay from E-G.

The lanthanide transporters **22** and **23** were compared to the corresponding free lanthanide ions. The complexes were formed by adding 0.9 eq of $LnCl_3 \times 6H_2O$ to the aqueous peptoid solution. The peptoid was used in excess to avoid uncomplexed lanthanide ions in the solution. It revealed that the lanthanide salts and the two peptoid complexes are able to pass the cell membrane (Figure 6), so that lanthanides can in principle act as a biomarker. Due to the low extinction coefficients of the lanthanides, the signal in each case was rather weak. Based on the cell images it is hard to say, if the transporters are more feasible biomarkers than the free lanthanides. But from our *in vitro* experiments (see Figure 3) we know, that the complexation with the peptoid raises the luminescence of the lanthanides. To amplify this finding, we started to introduce a so called antenna ligand into our peptoids, which is known for raising the extinction coefficients of the lanthanides. Concluding we are very confident, that the described lanthanide transporters are useful as luminescent probes. Furthermore we will test in the near future the gadolinium complexes as a contrast agent for magnet resonance tomography (MRT).

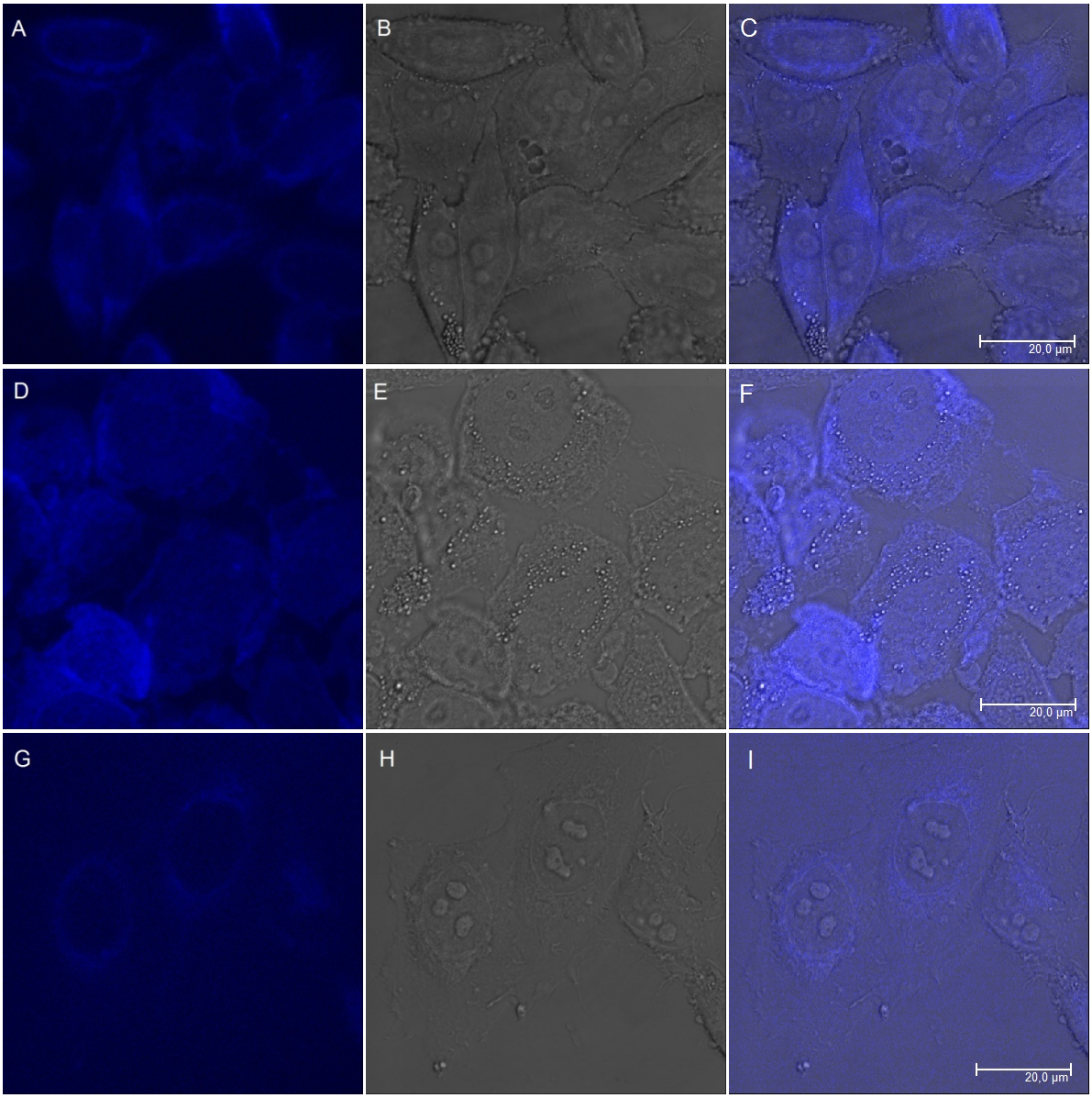

Figure 6: Confocal cell images (blue channel, differential interference contrast (DIC) channel and overlay) of HeLa cells, which were incubated with terbium(III) chloride and terbium transporters respectively. A-C 24 h incubation, 10 µM, $TbCl_3 \times 6H_2O$. D-F 24 h incubation, 10 µM, Tb^{3+} complex of **22**. G-I 24 h incubation, 10 µM, Tb^{3+} complex of **23**.

In cooperation with the working group of P. Roesky (see C1.06) three structurally identical lanthanide complexes, which contain the monomeric peptoid **25**, were synthesized (Figure 7). The 15 trivalent lanthanide ions are arranged around a central chloride ion, which might have a template effect. The complex periphery consists of 10 peptoid ligands **25** and 10 dibenzoylmethanide ligands (**26**).

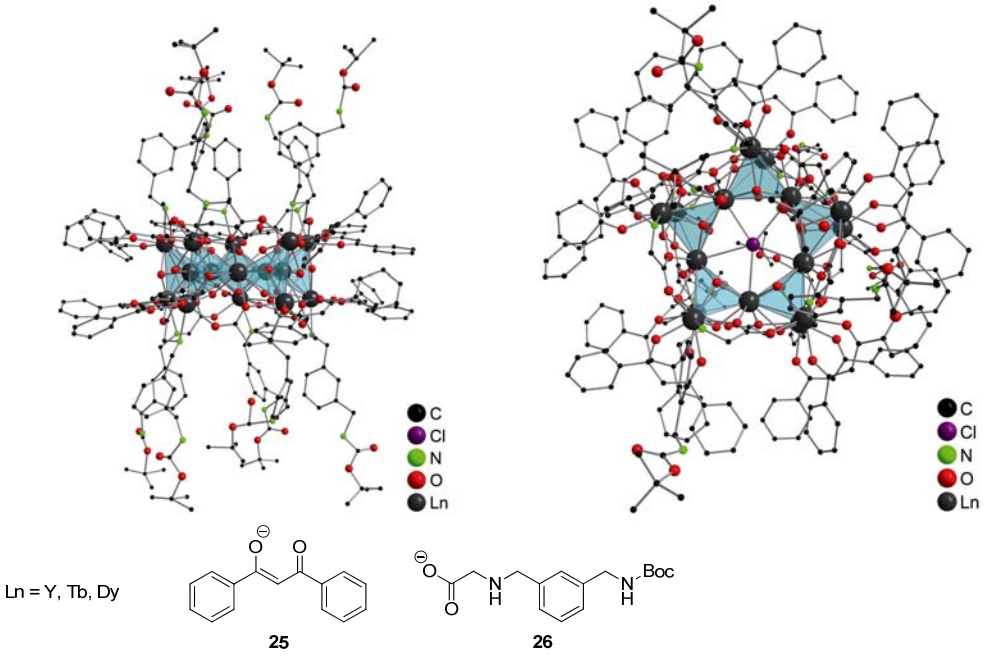

Figure 7: Side view (left) and front view (right) of the complex $[Ln_{15}(OH)_{20}(C_{15}H_{21}N_2O_4)_{10}(C_{15}H_{11}O_2)_{10}Cl]Cl_4$. The complex consists of 15 lanthanide ions (Y, Dy or Tb), 20 hydroxide ions, 10 monomeric peptoid ligands **25**, 10 DBM (**26**) ligands and one centered chloride ion. For a better overview the hydrogen atoms and non-coordinating chloride ions are not shown.

Since the spectroscopic features of these complexes are very promising, we tested them on HeLa cells (Figure 8). Due to the fact, that these complexes hold many lanthanide ions in small spaces, their luminescence has a higher intensity than comparable mononuclear complexes. But it turned out, that the complexes only possess poor water solubility. This corresponds to the relatively high cytotoxicity we found within our experiments. We tried to deprotect the amines of the peptoid ligands, which would provide a better solubility in water, but we observed only decomposition. By this time we are trying to synthesize analogue complexes with more polar and thus more water soluble ligands.

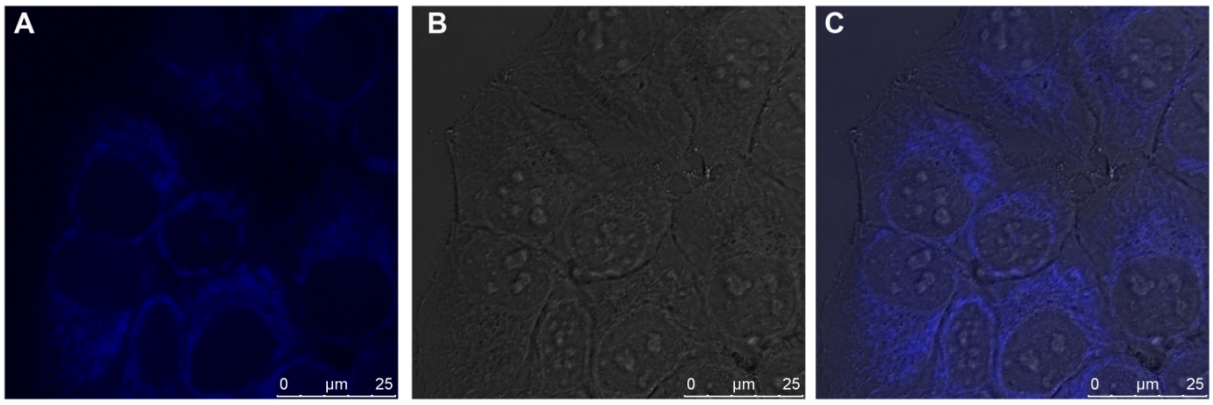

Figure 8: Confocal cell images of HeLa cells, which were incubated for 24 h with 1 µM dysprosium complex. A: blue channel. B: DIC channel. C: overlay of A and B.

3.2. Transport into plant cells

The transporter **25** was tested on tobacco cells. Using MitoTracker, we were able to show, that **25** is localized within the mitochondria. Since the mitochondria are partially moving very fast, we used the Zeiss Cell Observer SD for imaging. A 4D cell scan was taken (xyzt-time laps). In the *extended focus* mode the red marked mitochondria can be followed along the green actin filament. The original data were rendered by the software Imaris. That way, the mitochondria can be easily tracked within the whole cell. Figure 9 shows the tracking of one mitochondrion, which is colored yellow for a better overview, on its way through the cell.

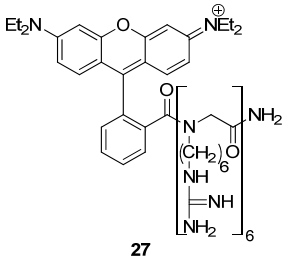

27

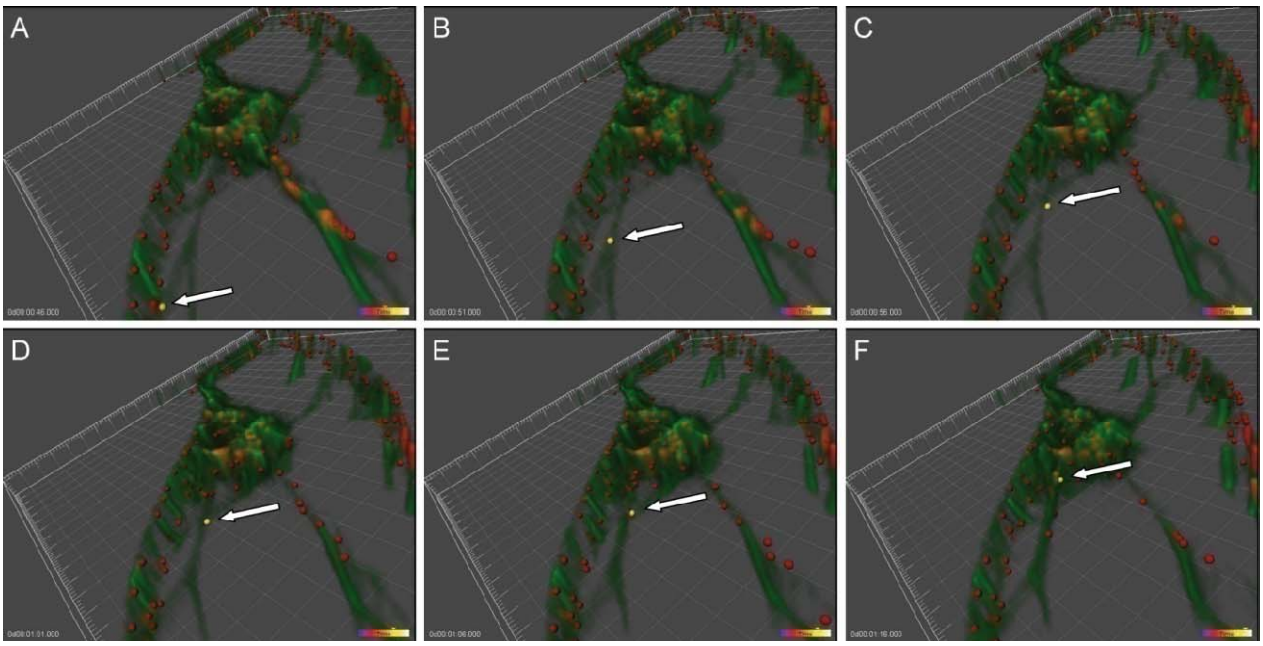

Figure 9: The arrows point at one single, yellow marked mitochondrion, which moves along an actin filament (A-F). The original microscopy data were rendered by the software Imaris. Tobacco BY-2, GFP marked actin filaments, incubated with **27**, 1 µM, 2 h incubation, Zeiss Cell Observer SD.

3.3. *In vivo* experiments

The porphyrin dye containing molecules **28** and **29** were tested on mice. An interesting fact is that emission spectrum of the porphyrin dye is highly affected by the structure of the transporter. Because of this, the peptoid transporter shows a red and the polyamine transporter a green fluorescence. Peptoid **28** showed an accumulation in the liver while polyamine **29** is targeted to lung and heart (Figure 10).

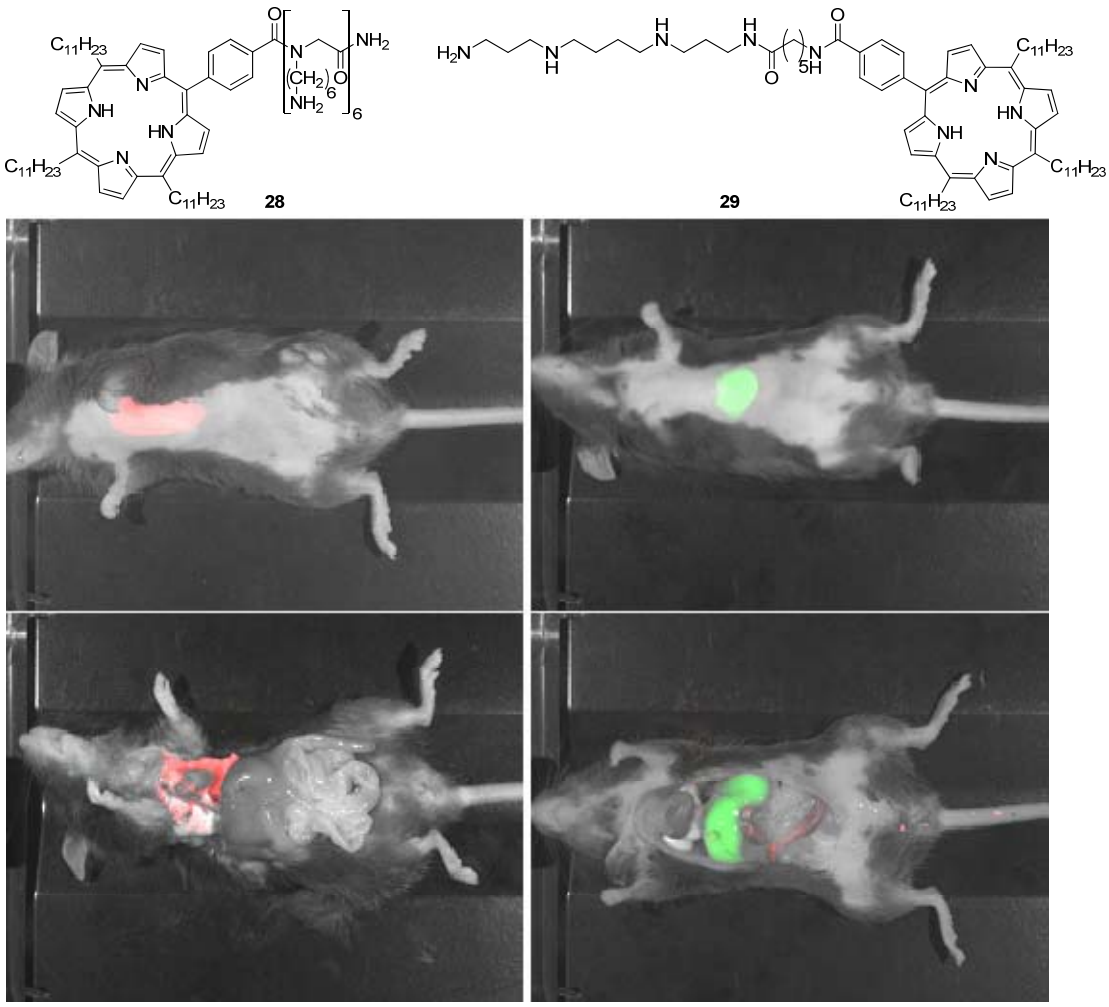

Figure 10: Comparison of the two porphyrin transporters **28** and **29**. Although they bear the same lipophilic porphyrin, their emission after excitation at the same wavelength is different (first row). After injection into mice, the conjugates accumulate in different organs. While **28** appears mainly in the lungs (left side), **29** was mainly found in the liver (right side).

4. Elucidation of Transport Mechanism

The pyridinium dye transporter **24** was used for a single organelle tracking. HeLa GFP-cells were incubated with **24** and afterwards a xyzt-time laps 4D scan, which gave an *extended focus* image, was taken (Figure 11). The red, endosomal structures can be clearly identified. They moved with different velocities. One very fast moving vesicle is tagged with arrows. The records were possible due to the special technical equipment of the Zeiss Cell Observer SD. It provides a spinning disc unit, which allows taking images with a notably high resolution. Additionally, these images were rendered with the software Imaris.

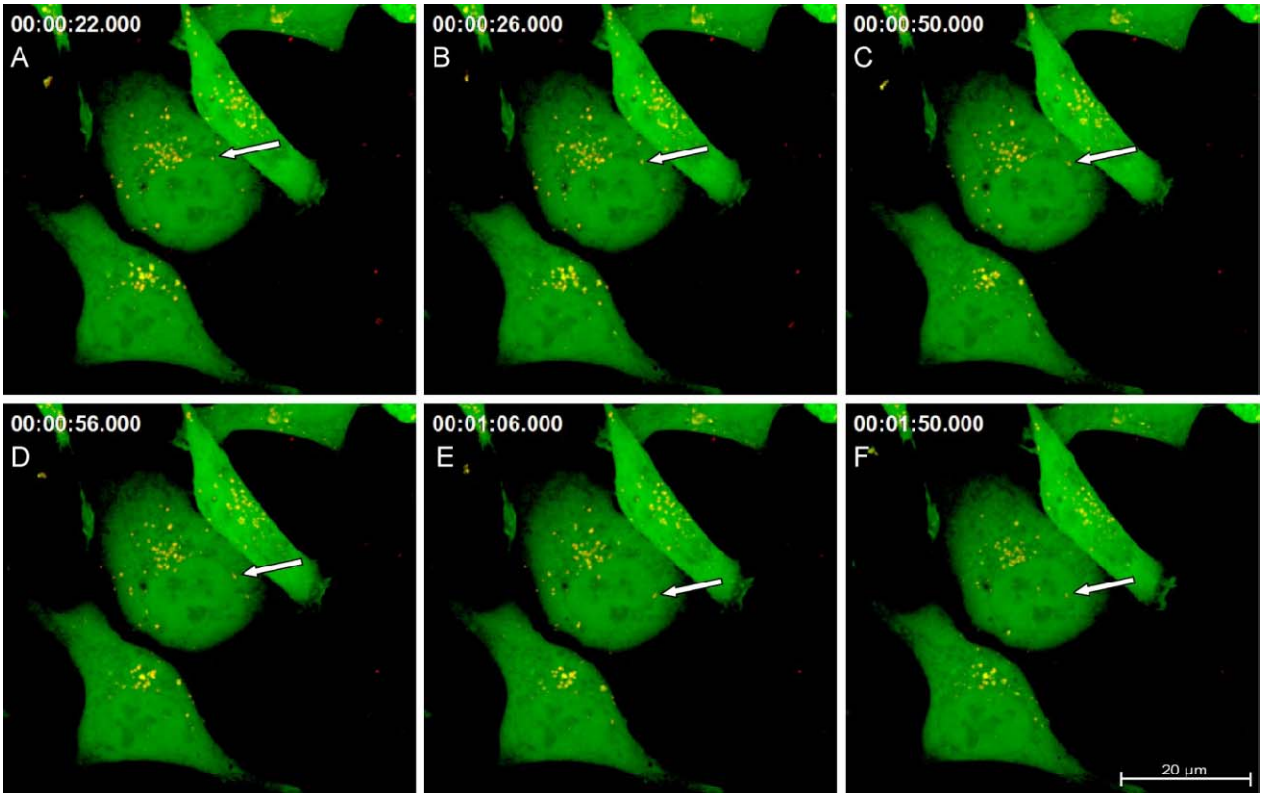

Figure 11: HeLa GFP-cells were incubated with **24**. A-F xyzt-timelapse, *extended focus* imaging, HeLa-GFP, 20 µM, 18 h incubation, Zeiss Cell Observer SD. The arrows point on a vesicle, which moves through the cell.

References

[1] S. Bräse, C. Gil, K. Knepper, and V. Zimmermann, *Organic Azides: An exploding variety of a unique class of compounds*, Angew. Chem. **117**, 5320 (2005); Angew. Chem. Int. Ed. **44**, 5188 (2005)

[2] * K.-H. Merz, T. Muller, S. Vanderheiden, G. Eisenbrand, D. Marko, and S. Bräse, *An efficient Synthesis of a Lycobetaine-Tortuosine Analogue – A Potent Topoisomerase Inhibitor, Synlett*, 3461 (2006)

[3] * T. Schröder, K. Schmitz, N. Niemeier, T. S. Balaban, H. F. Krug, U. Schepers, and S. Bräse, *Solid-Phase Synthesis, Bioconjugation, and Toxicology of Novel Cationic Oligopeptoids for Cellular Drug Delivery*, Bioconjugates **18**, 342 (2007)

[4] T. Schröder, M. Gartner, T. Grab, and S. Bräse, *A new azide staining reagent based on "click" chemistry*, Org. Biomol. Chem. **5**, 2767-2769 (2007)

[5] * T. Schröder, A. Quintilla, J. Setzler, E. Birtalan, W. Wenzel, and S. Bräse, *Joint experimental and theoretical investigation of the propensity of peptoids as drug carriers,* WSEAS Trans. Biol. Biomed. **4** (9), 120 (2007)

[6] N. Jung, M. Wiehn, and S. Bräse, Springer, Heidelberg. *Multifunctional linkers for diversity-oriented solid phase syntheses Top. Curr. Chem*. (2007)

[7] F. Hahn and U. Schepers, *Solid Phase Chemistry for the Directed Synthesis of Biologically Active Polyamine Analogs, Derivatives, and Conjugates*. In: Bräse S (ed) Combinatorial Chemistry on Solid Supports, vol 278. Springer Verlag, Berlin, Heidelberg, p 135 (2007)

[8] S. Bräse, Guest editor, *Top. Curr. Chem*., Springer, *Combinatorial Chemistry on Solid Supports,* (2007)

[9] * T. Schröder, N. Niemeier, H. F. Krug, S. Afonin, A. Ulrich, and S. Bräse, *Peptoidic amino- and guanidinium-carrier systems: targeted drug delivery into the cell cytosol or the nucleus*, J. Med. Chem. **51**, 376 (2008)

[10] * F. Hahn, K. Schmitz, T. S. Balaban, S. Bräse, and U. Schepers, *Conjugation of Spermine Facilitates Cellular Uptake and Enhances Antitumor and Antibiotic Properties of Highly Lipophilic Porphyrins,* ChemMedChem **3**, 1185 (2008)

[11] * K. Eggenberger, T. Schröder, E. Birtalan, A. Merkoulov, M. Darbandi, T. Nann, S. Bräse, and P. Nick, *The use of nanoparticles to study and manipulate the polarity of plant cells,* Eur. J. Cell. Biol. **87**, 62, Suppl. 58 (2008)

[12] M. Wiehn, N. Jung, and S. Bräse, in The Power of Functional Resins in Organic Chemistry, F. Albercio, J. Tulla (Eds.), Wiley-VCH, 2008, 437-465. *Safety-Catch and Traceless Linkers* (2008)

[13] F. Hahn, and U. Schepers, *Versatile procedure for asymmetric and orthogonal protection of symmetric polyamines and its advantages for solid phase synthesis*. J Comb Chem 10: 267 (2008)

[14] * U. Schepers, K. Schmitz, and S. Bräse, *Smart Vehicles for Drug Delivery: Molecular Transporters and Trojan Peptides for Fast Delivery*, invited review for Angew. Chem., submitted

[15] F. Hahn, K. Müllen, and U. Schepers, *2-Iminothiolane as a useful coupling reagent for polyamine solid phase synthesis*, Synlett **18**, 2785 (2008)

[16] E. Birtalan, D. Fritz, L. Hammerich, A. Frintrup, F. Hahn, P. Knüfermann, S. Bräse, and U. Schepers, *Amphipathic peptoid transporters with aromatic side chains can be exploited for mitochondrial delivery of therapeutic drugs*, in preparation

[17] A. Frintrup, F. Hahn, A. Carstensen, P. Knüfermann, and U. Schepers, *Kinetics of cellular uptake and toxicology of polyamine based molecular transporters by HPLC and fluorometric assays*, Chem. Res. Toxicol. submitted

[18] T. Mack, F. Hahn, and U. Schepers, *Copper(I)-catalyzed Huisgen [2+3]-cycloaddition reactions facilitates the covalent coupling of carbohydrates and nucleic acids to polyamine moieties on solid supports*, in preparation

[19] K. Schmitz, F. Hahn and U. Schepers, *Modified GSMP synthesis greatly improves the disulfide crosslink of T7 run-off siRNAs with cell penetrating peptides*, Synlett accepted (2010)

[20] * K. Eggenberger, T. Schröder, E. Birtalan, S. Bräse, and P. Nick, *Passage of Trojan Peptoids into Plant Cells.* ChemBioChem **10***,* 2504-2512 (2009)

[21] D. Fritz, and S. Bräse, *Solid-phase synthesis of ω-aminoalkylpeptoids using azide chemistry.* Synlett, 1544 (2010)

[22] * B. Rudat, E. Birtalan, I. Thomé, D. K. Kölmel, V. L. Horhoiu, M. D. Wissert, U. Lemmer, H.-J. Eisler, T. S. Balaban, and S. Bräse, *Novel pyridinium dyes that enable investigations of peptoids at the single-molecule level,* J. Chem. Phys. B **114**, 13473-13480 (2010)

[23] * E. Birtalan, K. Eggenberger, O. Lemke, I. Hebeiss, C. Bednarek, J. Sieber, P. Nick, U. Schepers, and S. Bräse, *Mitochondria-Penetrating Peptoids as Tool to Analyze Actin-Dependent Mitochondrial Movements by High Speed 4D-Confocal Microscopy in Plant Cells.* PLoS ONE, accepted (2011)

[24] * E. Birtalan, A. Frintrup, C. Bednarek, P. Sieber, P. Knüfermann, K. Müllen, S. Bräse, and U. Schepers, *Amphiphilic peptoid Transporters can be Exploited for Mitochondrial Delivery of Therapeutic Drugs.* J. Biol. Chem., submitted (2010)

[25] E. Birtalan, B. Rudat, D. K. Kölmel, D. Fritz, S. B. L. Vollrath, and S. Bräse, *Investigation of Spirolactam Formation of Rhodamine B-labelled Peptoids and its Scopes and Limitations for in vitro Applications.* Biopolym. Pept. Sci., in revision (2010)